



A QM/MM study of the molecular recognition site of bapineuzumab toward the amyloid- β peptide isoforms

Lucas J. Gutierrez, Exequiel E. Barrera Guisasola, Nelida Peruchena & Ricardo D. Enriz


To cite this article: Lucas J. Gutierrez, Exequiel E. Barrera Guisasola, Nelida Peruchena & Ricardo D. Enriz (2016) A QM/MM study of the molecular recognition site of bapineuzumab toward the amyloid- β peptide isoforms, *Molecular Simulation*, 42:3, 196-207, DOI: [10.1080/08927022.2015.1032276](https://doi.org/10.1080/08927022.2015.1032276)

To link to this article: <http://dx.doi.org/10.1080/08927022.2015.1032276>

 View supplementary material 

 Published online: 28 Apr 2015.

 Submit your article to this journal 

 Article views: 58

 View related articles 

 View Crossmark data 

A QM/MM study of the molecular recognition site of bapineuzumab toward the amyloid- β peptide isoforms

Lucas J. Gutierrez^a, Exequiel E. Barrera Guisasola^{b,c}, Nelida Peruchena^a and Ricardo D. Enriz^{b,c*}

^aLaboratorio de Estructura Molecular y Propiedades, Área de Química Física, Departamento de Química, Facultad de Ciencias Exactas y Naturales y Agrimensura, Universidad Nacional del Nordeste, Avda. Libertad 5460, (3400) Corrientes, Argentina; ^bFacultad de Química, Bioquímica y Farmacia, Universidad Nacional de San Luis, Chacabuco 915, (5700) San Luis, Argentina; ^cInstituto Multidisciplinario de Investigaciones Biológicas (IMIBIO-SL -CONICET), Chacabuco 915, (5700) San Luis, Argentina

(Received 9 November 2014; final version received 17 March 2015)

The molecular mechanism of recognition of amyloid-beta ($A\beta$) peptide isoforms by bapineuzumab was studied using a quantum mechanics and molecular mechanics (QM/MM) method. In this work, geometric optimisations were performed using the ONIOM2 scheme (at B3LYP/6-31G(d) amberEE level) on the paratope of bapineuzumab together with the different forms of $A\beta$ peptide ($A\beta_{WT}$ and $A\beta_{N3(pE)}$). A comprehensive study of the interactions was also performed through Quantum Theory of Atoms in Molecules (QTAIM). This allowed us to obtain a deep understanding of how this antibody interacts with the amino acids of the $A\beta$ peptides. The description on the interactions between bapineuzumab and the different forms of $A\beta$ peptides allow us to understand why the peptides that lack the two first residues (Asp1 and Ala2) and begin with a pyroglutamate residue present low affinity for bapineuzumab. This basic structural information is useful for a deeper understanding about the scope and limitations of bapineuzumab as a therapeutic agent for the AD.

Keywords: Alzheimer's disease; amyloid-beta peptide; ONIOM calculations; QTAIM analysis

1. Introduction

Alzheimer's disease (AD) is the most prevalent neurodegenerative disease in humans. It is a genetically complex, slowly progressive, and irreversible disease of the brain. Besides, it is one of the most common causes of mental deterioration in elderly people, accounting for around 50–60% of the overall cases of dementia among persons over 65 years of age.[1] Currently, it is known that amyloid-beta ($A\beta$) peptides form soluble oligomers, which are key pathogenic structures in AD. They inhibit the synaptic function, leading to early memory deficits and synaptic degeneration. The soluble $A\beta$ oligomers in the hippocampal neurons trigger hyperphosphorylation of tau, a key step in the generation of neurofibrillary tangles.[2,3] Because of these effects, the soluble $A\beta$ oligomers represent an attractive therapeutic target.

Immunotherapy has become a very attractive alternative as a new treatment for brain disorders. This is because the antibodies are highly selective. Recently, a humanised monoclonal antibody, called bapineuzumab, was reported. This antibody binds with high affinity to the neurotoxic free N-terminal $A\beta$ peptides ($A\beta_{WT}$).[4] Clinical trials in patients with moderate AD show that bapineuzumab was effective in stabilising amyloid plaque burden and lowering phosphorylated-tau levels in cerebrospinal fluid.[4] Despite these promising results, immunotherapy fails to improve the cognitive ability of patients.

In addition to the $A\beta_{WT}$ peptides present in the human brain, there are $A\beta$ peptides N-terminal truncated in the residues Glu3 ($A\beta_{N3(pE)}$) and Glu11 ($A\beta_{N11(pE)}$).[5–7] These modified peptides are resistant to aminopeptidases, which justifies its abundance in brain tissue.[8] Studies of circular dichroism show a faster aggregation kinetics than $A\beta_{WT}$ peptides.[9] In turn, Nussbaum et al. [10] demonstrated that $A\beta_{N3(pE)}$ may form low molecular weight hybrid oligomers with the full-length $A\beta_{WT}$ peptide and cause an accelerated misfolding and oligomerisation of $A\beta_{WT}$ leading to toxic structures. Among these species, $A\beta_{N3(pE)}$ is a major N-truncated constituent of intracellular, extracellular and vascular $A\beta$ deposits in AD brain tissue.[11]

A possible explanation of bapineuzumab failure in cognitive improvement of AD patients is that the N-terminal modified peptides are the main component of senile plaques, which constitute more than 50% of the $A\beta$ in neuritic plaques.[12] In turn, bapineuzumab presents low affinity on these N-terminal modified $A\beta$ -peptides found in amyloid deposits with respect to the $A\beta_{WT}$ peptides.[4] The sum of these factors might be the cause of the lack of bapineuzumab efficacy in the treatment of AD.[8]

Although there are different factors responsible for bapineuzumab failure as a therapeutic agent against AD, [13,14] the hypothesis raised by Perez-Garmendia and Gevorkian [8] should be taken into account since it

*Corresponding author. Email: denriz@unsl.edu.ar

is very interesting and well-founded. Furthermore, it has been reported that Bapinezumab has less affinity for the A β N-terminal modified with respect to A β_{WT} . [4] Therefore, the question that arises is: what is the cause of this different affinity? Actually, the problem is that there is no precise information at molecular level of the interaction types that stabilise and/or destabilise these two complexes. It is evident that a detailed analysis of the different molecular interactions in the binding process is of paramount importance.

The main objective of this study is to investigate the interactions between the A β peptide isoforms (A β_{WT} and A $\beta_{N3(pE)}$) and bapinezumab using computational calculations. This study might allow us to better understand how this antibody interacts with the amino acid residues of the different A β peptides. This basic structural information can be useful for a deeper understanding about the scope and limitations of bapinezumab as a therapeutic agent for the AD. On the other hand, this information might be also useful to improve the therapeutic effect of novel monoclonal antibodies anti-A β peptide.

2. Methods and computational details

2.1. Antibody-A β_{WT} peptide model (Ab-A β_{WT})

Coordinates of bapinezumab Fab fragment (2.2 Å resolution) complexed to the A β_{WT} peptide were downloaded from protein data bank (PDBcode:4HIX). [4] The residues 7–28 of A β_{WT} peptide were located outside the paratope region and had high mobility; thus they were not in the crystallographic structure. [4] Anyway this was not a problem for the studies performed here since only residues 1–6 were involved in the bonding process (Figure 1(a)). Finally, antibody Fab fragment together with A β_{WT} (residues 1–6) and crystal water molecules were the source of initial coordinates for our model system.

2.2. Antibody-A $\beta_{N3(pE)}$ peptide system (Ab-A $\beta_{N3(pE)}$)

This system was built from the same geometry that was used in the above model in which the N-terminus was replaced by pyro-Glu3 (Figure 1(b)). The root-mean-square deviations (RMSD) of C $_{\alpha}$ for residues 3–6 between

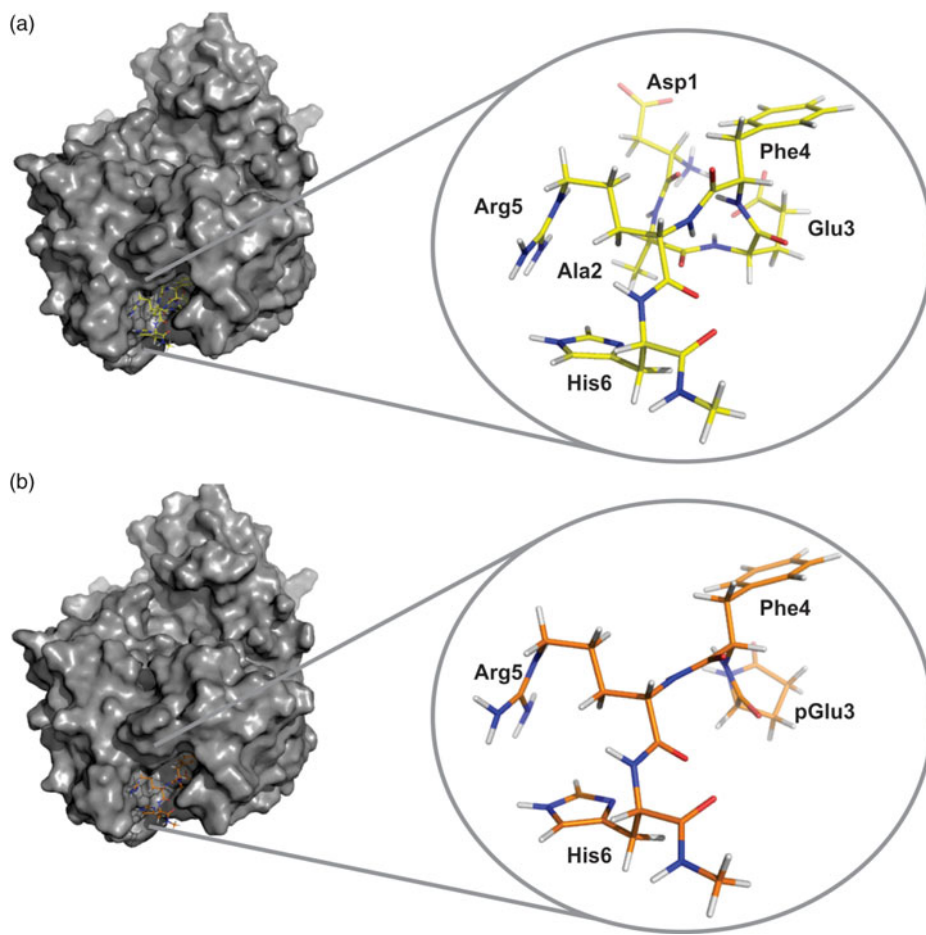


Figure 1. (Colour online) Surface representation of the antibody binding region. Molecular structure of (a) A β_{WT} peptide (yellow) and (b) A $\beta_{N3(pE)}$ peptide (orange).

$A\beta_{WT}$ and $A\beta_{N3(pE)}$ was only 0.12 Å, concordantly with the values previously reported by Gardberg et al. [15].

2.3. Molecular dynamics

Molecular dynamics simulations (MD) and subsequent structural analysis were performed with the Amber12 package.[16] The all-atom force field ff99SB [17] was used to describe the complexes, whereas the water molecules were represented using the TIP3P model. Each model was soaked in a truncated octahedral periodic box of TIP3P water molecules. The distance between the edges of the water box and the closest atom of the solutes was at least 10Å. Chloride ions were added to neutralise the charge of the system. The entire system was subject to energy minimisation in two stages in order to remove bad contacts between the complex and the solvent molecules. First, the water molecules were minimised by keeping the solute fixed with harmonic constraint with a force of 100 kcal/molÅ². Second, conjugate gradient energy minimisations were performed repeatedly four times using the positional restraints to all heavy atoms of the complexes with 15, 10, 5 and 0 kcal/molÅ². The values of RMSD between the initial and minimised structures were lesser than 0.5 Å.

In the next place each system was then heated in the NVT ensemble from 0 to 300 K in 500 ps and equilibrated at an isothermal isobaric (NPT) ensemble for another 500 ps. A Langevin thermostat [18] was used for temperature coupling with a collision frequency of 1.0 ps⁻¹. The particle mesh Ewald (PME) method was employed to treat the long-range electrostatic interactions in a periodic boundary condition.[19] The SHAKE method was used to constrain hydrogen atoms. The time step for all MD is 2 fs, with a direct-space, non-bonded cutoff of 8 Å. Finally, the production was carried out at the NPT conditions performing simulations of 30 ns in length for each system.

2.4. Aβ-Residue interaction decomposition

The interactions between the Aβ peptide and each residue in the paratope were calculated using the MM/GBSA decomposition programme implemented in AMBER 12. The interaction between Aβ peptide–residue pairs is approximated by:

$$\Delta G_{A\beta\text{-residue}} = \Delta G_{vdw} + \Delta G_{ele} + \Delta G_{GB} + \Delta G_{SA}, \quad (1)$$

where ΔG_{vdw} and ΔG_{ele} are non-bonded van der Waals interactions and electrostatic interactions between the Aβ peptide and each paratope residue in the gas phase. The polar contribution to solvation free energy (ΔG_{GB}) was calculated using the GB module.[20] ΔG_{SA} is free energy due to the solvation process of nonpolar contribution and was calculated from SASA. All energy components in Equation (1) were calculated using 1000 snapshots from the last 10 ns of the MD simulation.

2.5. QM/MM setup

The most important question when using the ONIOM scheme is the partitioning of the system into high and low level layers. In this work, we identified the paratope residues using the free energy decomposition approach (MM/GBSA). The side chains of the paratope residues that contributed with a $|\Delta G|$ higher than 1.0 kcal/mol in the per residue energy decomposition, the Aβ peptide and the water molecules were included at the high-level QM layer, and the remainder of the complex system was included in the low-level MM layer. The QM region was calculated using the B3LYP/6-31G(d) method and the MM portion using the AMBER force field.[21] The MM parameters absent in the standard AMBER force field were included from the generalised amber force field (GAFF).[22] Atoms in the QM region were optimised using the electrical embedding scheme. Hydrogen link atoms were used to satisfy atoms at the QM and MM interface. The hydrogen link atoms remained fixed during optimisation.

2.6. Binding energy calculations

The binding energies of the complex system were calculated as single-point calculations at B3LYP/6-31G(d) level of theory, including basis set superposition error (BSSE) corrections,[23,24] using the geometries obtained by QM/MM calculations. The binding energy ($\Delta E_{\text{binding}}$) of each complex can be defined as follows [25]:

$$\Delta E_{\text{binding}} = E_{\text{complex}} - E_{A\beta} - E_{\text{binding site}} + \text{BSSE}, \quad (2)$$

where E_{complex} is the complex (binding site-Aβ) energy, $E_{A\beta}$ and $E_{\text{binding site}}$ are the energies of the Aβ peptide, and binding site, respectively. All of these calculations were carried out with Gaussian 09 suite of programmes.[26]

2.7. Atoms in molecules theory

After the QM/MM calculation, the optimised geometry for each Aβ–antibody complexes (Ab–Aβ) was used as input for quantum theory atoms in molecule (QTAIM) analysis, [27] which was performed with the help of Multiwfn software,[28] using the wave functions generated at the B3LYP/6-31G(d) level.

3. Results and discussions

3.1. Equilibrium of the dynamics simulation

The RMSD of each snapshot relative to the initial structure was calculated to monitor the stability of each trajectory. Figures S1 and S2 in the supplemental material show the RMSD values for the backbone atoms of the complexes Ab–Aβ_{WT} and Ab–Aβ_{N3(pE)}. It is possible to observe that the RMSD of all the trajectories do not suffer

significant changes during the simulation. Thus, the average RMSD values obtained for Ab–A β _{WT} complex were 1.45 Å (V_H chain), 1.41 Å (V_L chain) and 0.40 Å (A β _{WT} peptide) with respect to the initial structure whereas for Ab–A β N3(pE), the average RMSD values were 1.95 Å (V_H chain), 1.72 Å (V_L chain) and 1.00 Å for A β N3(pE) peptide. These results are shown in Table S3 in the supplemental material. It should be noted that the backbone conformation of both peptides is substantially conserved during the 30 ns of simulation (see Figure S4 in supplemental material).

3.2. Determining the QM layer

In order to determine which amino acid residues are producing the A β –antibody association, we calculated the binding free energy $\Delta G_{\text{A}\beta\text{WT-residue}}$ and $\Delta G_{\text{A}\beta\text{N3(pE)-residue}}$. As shown in Figure 2(a), eight residues (V_H-Ser50, V_H-Arg52, V_H-Tyr95, V_H-Ser101A, V_H-Ser101B, V_L-Asp27D, V_L-Trp89, V_L-Arg96) make large contributions to the binding energy, providing free-energy contributions

of >2 kcal mol⁻¹. In addition, other five residues (V_H-Trp47, V_H-Tyr59, V_L-Asp28, V_L-Tyr32, V_L-Phe94) also make considerable contributions to the binding process between A β peptide and the antibody, each yielding >1 kcal mol⁻¹ of free energy. On the other hand, in Figure 2(b) only V_H-Tyr59, V_L-Asp27D, V_L-Asp28, V_L-Trp89 and V_L-Arg96 contribute to the free-energy with more than 1 kcal/mol. Therefore, the residues V_H-Trp47, V_H-Ser50, V_H-Arg52, V_H-Tyr59, V_H-Tyr95, V_H-Ser101A, V_H-Ser101B, V_L-Asp27D, V_L-Asp28, V_L-Tyr32, V_L-Phe94, V_L-Trp89 and V_L-Arg96 were selected to form part of QM layer together with the A β peptide and six water molecules that were found within the antibody paratope.

3.3. Analyses of the optimisations and binding energy

The agreement of the structures obtained from the geometric optimisations for the Ab–A β _{WT} and Ab–A β N3(pE) complexes with their respective initial structures was evaluated through a superimposition analysis. The RMSD between the initial and optimised

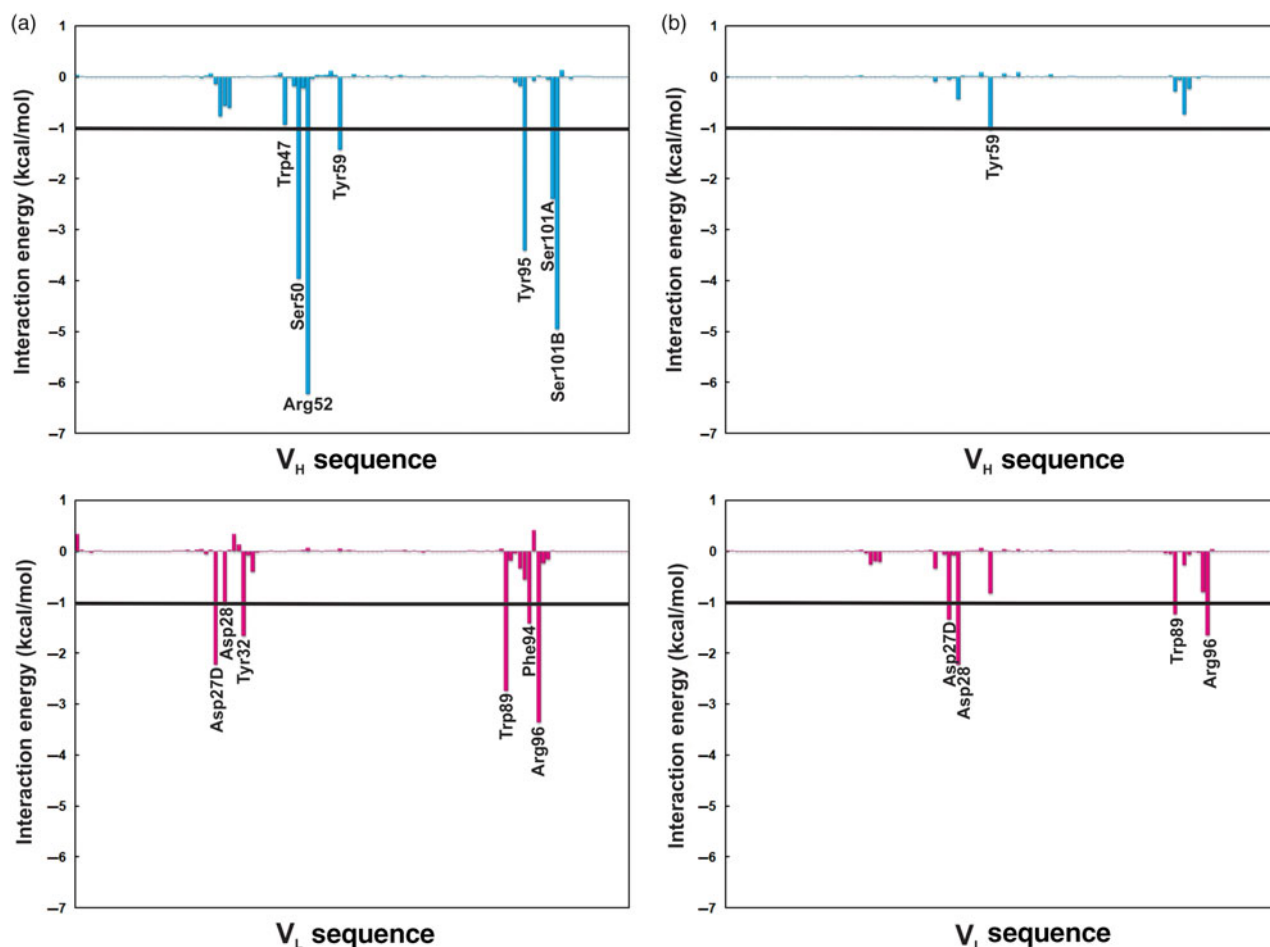


Figure 2. (Colour online) Interaction spectrum. The x-axis denotes the residue number of V_H and V_L chains of bapineuzumab for (a) A β _{WT} and (b) A β N3(pE). The y-axis denotes the interaction contribution energy of individual residues.

structures were 0.16 and 0.35 Å for Ab–A β _{WT} and Ab–A β N3(pE), respectively, which clearly indicates that the orientations and positions of the two complexes do not change significantly during the optimisation process.

A β _{WT} binds more tightly to the antibody with respect to A β N3(pE), being the gap between the binding energies 25.3 kcal/mol. Thus, it is encouraging that the ranking of the experimental binding energies is consistent with our calculations, which shows that the structures obtained from the ONIOM2 scheme are reliable.

3.4. Analysis of the interactions network of residues using QTAIM calculations

The QTAIM analysis is very important in the study of ligand–receptor interactions because the values of the electronic density ($\rho_{(r)}$) at a critical point bond (CPB) indicate the strength of the interactions. Therefore, the sum of the values of $\rho_{(r)}$ for each interaction individually will give us a better understanding and more detailed information on the mode of binding between bapineuzumab and the different A β forms.

3.4.1. Key residues in the paratope region

To understand why bapineuzumab has lower affinity for A β N3(pE) than for A β _{WT}, an exhaustive analysis of Figure 3 will be helpful. This figure shows the electronic density located in the BCP for the different interactions obtained for Ab–A β _{WT} and Ab–A β N3(pE). Here it might be appreciated that the sum of $\rho_{(r)}$ for Ab–A β _{WT} is 1.001 u.a., which is greater with respect to Ab–A β N3(pE) ($\rho_{(r)}$ = 0.773 u.a.), indicating a preference of bapineuzumab for A β _{WT}. This result is in agreement with our calculated binding energy and the previously reported experimental data.[4]

It should be noted that RMSD for the C α of residues 3–6 of A β _{WT} and A β N3(pE) is only 0.14 Å. However, Figure 3 shows that the replacement of Glu by pyro-Glu has a drastic effect on the bind, which is reflected in the loss of interactions. Comparing Figure 3(a),(b), it is possible to appreciate lower values of $\rho_{(r)}$ for Ab–A β N3(pE) in several interactions. Furthermore, this figure also shows that six residues (V_H-Ser50, V_H-Arg52, V_H-Tyr95, V_H-Ser101B, V_L-Asp27D and V_L-Arg96) make large contributions to the binding between the different forms of A β peptide and bapineuzumab, giving values of $\rho_{(r)}$ > 0.04 u.a.

Analysing residue by residue in Figure 3, it is possible to observe a difference for V_H-Ser50. The interaction OH_{V_H-Ser50}...O_{A β WT-Glu3} (Figure 4(a)) ($\rho_{(r)}$ = 0.0429 u.a. green colour) is stronger than OH_{V_H-Ser50}...O_{A β N3(pE)-pGlu3} ($\rho_{(r)}$ = 0.0285 u.a.) (Figure 4(b)) because the formation of the ring makes the distance OH...O greater in Ab–A β N3(pE) than in Ab–A β _{WT}.

In addition, V_H-Arg52 is one of the most important residues of the paratope of bapineuzumab. From Figure 5 can appreciate that in both cases V_H-Arg52 is making the following interactions: HH11_{V_H-Arg52}...O_{A β WT/A β N3(pE)-Phe4}, HH22_{V_H-Arg52}...O_{A β WT/A β N3(pE)-His6}, HE_{V_H-Arg52}...O_{A β WT/A β N3(pE)-Glu3/p-Glu3} and several interactions CH...CH.

Another key residue involved in the recognition of A β peptides is V_H-Tyr95. As seen in Figure 6 in both complexes V_H-Tyr95 has several hydrophobic interactions with Phe4. However, the interaction OH_{V_H-Tyr95}...HG3_{A β WT/A β N3(pE)-Arg5} is stronger in the Ab–A β _{WT} complex because the atoms involved in the interaction are closer.

In the Ab–A β _{WT} complex, V_H-Ser101B produces two strong hydrogen bonds with Asp1 (H_{V_H-Ser101B}...OD2_{A β WT-Asp1} and HG_{V_H-Ser101B}...OD1_{A β WT-Asp1} (Figure 7). It should be noted that Asp1 is missing in A β N3(pE)

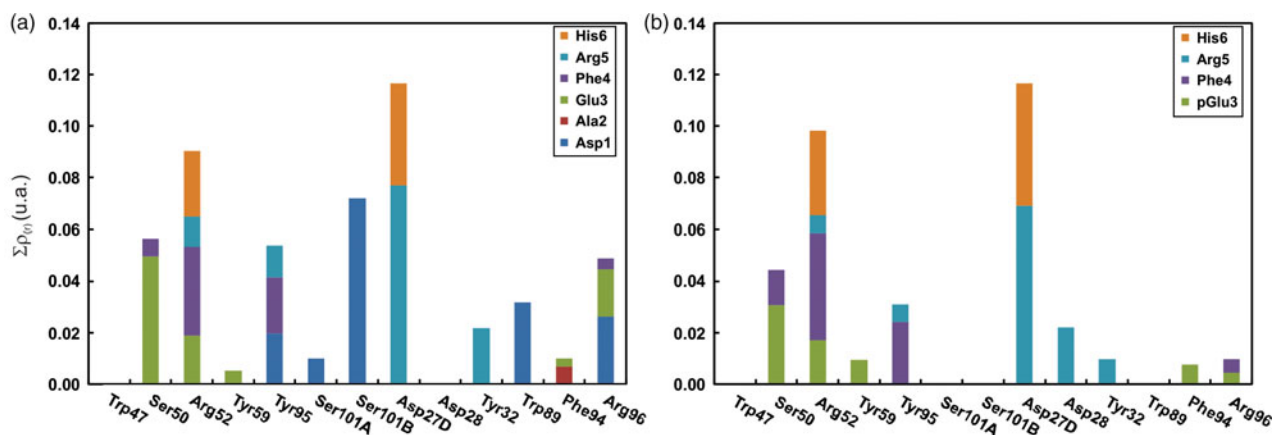


Figure 3. (Colour online) Sum of the values of charge density ($\Sigma\rho_{(r)}$) at the bond critical points (considering only the intermolecular interactions) in (a) Ab–A β _{WT} and (b) Ab–A β N3(pE).

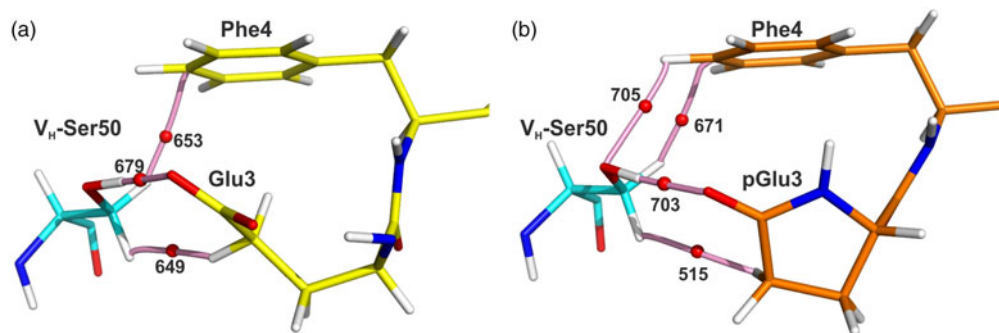


Figure 4. (Colour online) Molecular graph of the noncovalent interactions between the paratope residue (V_H -Ser50) of bapineuzumab and (a) the residues Glu3-Phe4 of $A\beta_{WT}$ peptide (b) the residues pGlu3-Phe4 of $A\beta_{N3(pE)}$ peptide. Also the elements of the topology of the electron density are shown: pink spheres represent the bond paths connecting the nuclei and the critical bond points are represented as red spheres. The ID of each BCP is shown in this figure in order to obtain more details about the interactions in the supplemental material (see Table S5 and Table S6).

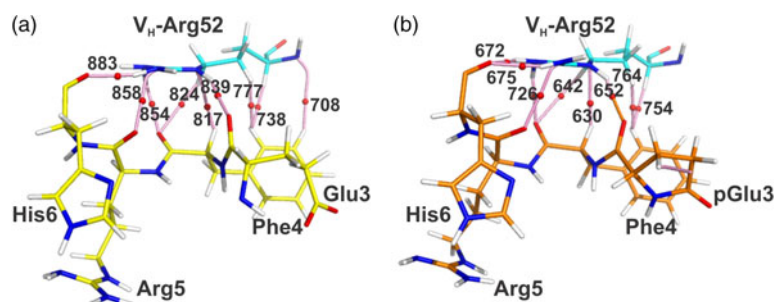


Figure 5. (Colour online) Molecular graph showing the noncovalent interactions between the paratope residue (V_H -Arg52) of bapineuzumab and (a) the residues Glu3-Phe4-Arg5-His6 of $A\beta_{WT}$ peptide (b) the residues pGlu3-Phe4-Arg5-His6 of $A\beta_{N3(pE)}$ peptide.

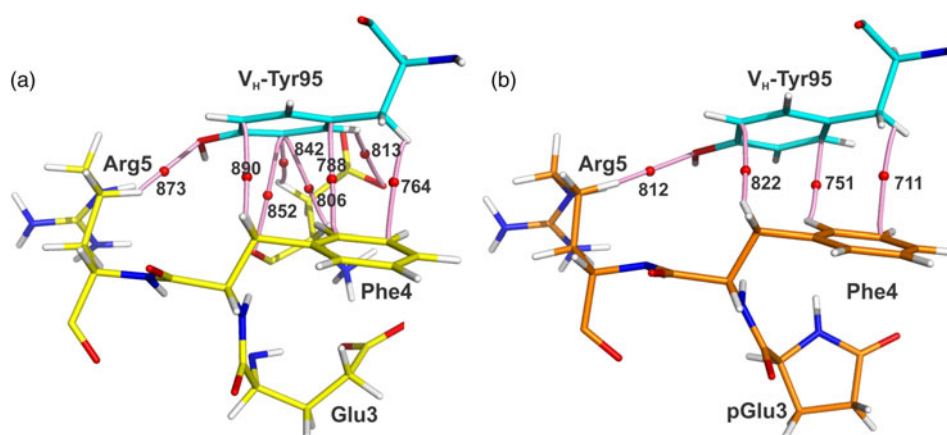


Figure 6. (Colour online) Molecular graph of the noncovalent interactions between the paratope residue (V_H -Tyr95) of bapineuzumab and (a) the residues Glu3-Phe4-Arg5 of $A\beta_{WT}$ peptide (b) the residues pGlu3-Phe4-Arg5 of $A\beta_{N3(pE)}$ peptide.

which might explain, at least in part, the low affinity of the antibody for the $A\beta_{N3(pE)}$ peptide.

The residue V_H -Asp27D of Bapineuzumab produces strong interactions with Arg5 and His6 of both peptides ($A\beta_{WT}$ and $A\beta_{N3(pE)}$). In Ab- $A\beta_{WT}$, the

oxygen OD1 of carboxylate group of V_H -Asp27D is forming three hydrogen bonds ($OD1_{V_H-Asp27D} \cdots HH12_{A\beta_{WT}-Arg5}$, $OD1_{V_H-Asp27D} \cdots HH22_{A\beta_{WT}-Arg5}$ and $OD1_{V_H-Asp27D} \cdots HE2_{A\beta_{WT}-His6}$), while that in Ab- $A\beta_{N3(pE)}$, the oxygen OD1 of V_H -Asp27D has two hydrogen

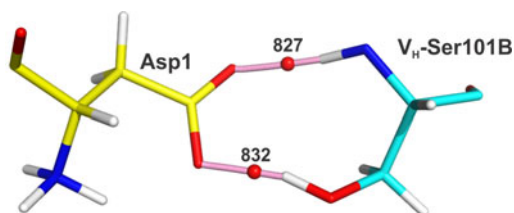


Figure 7. (Colour online) Molecular graph of the noncovalent interactions between the paratope residue (V_H -Ser101B) of bapineuzumab and the residues Asp1 of $A\beta_{WT}$ peptide.

bonds ($OD1_{VH-Asp27D} \cdots HH22_{A\beta N3(pE)-Arg5}$ and $OD1_{VH-Asp27D} \cdots HE2_{A\beta N3(pE)-His6}$) and OD2 acts as H-acceptor with Arg5 ($OD2_{VH-Asp27D} \cdots HH12_{A\beta N3(pE)-Arg5}$) (Figure 8).

Figure 9(a) shows a large number of interactions between V_L -Arg96 and Asp1 while the residues Glu3/pGlu3 and Phe4 present only two interactions with V_L -Arg96 (Figure 9(a),(b)). This clearly indicates that the preference of bapineuzumab for $A\beta_{WT}$ is mainly due to the residue Asp1.

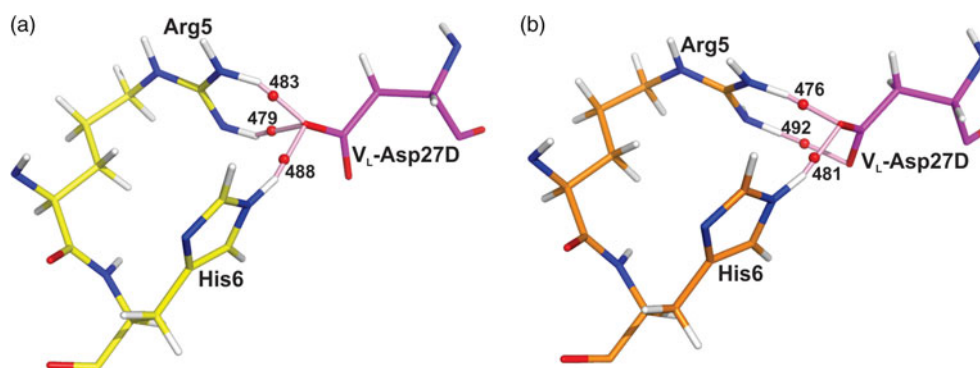


Figure 8. (Colour online) Molecular graph of the noncovalent interactions between the paratope residue (V_L -Asp27D) of bapineuzumab and (a) the residues Arg5-His6 of $A\beta_{WT}$ peptide (b) the residues Arg5-His6 of $A\beta N3(pE)$ peptide.

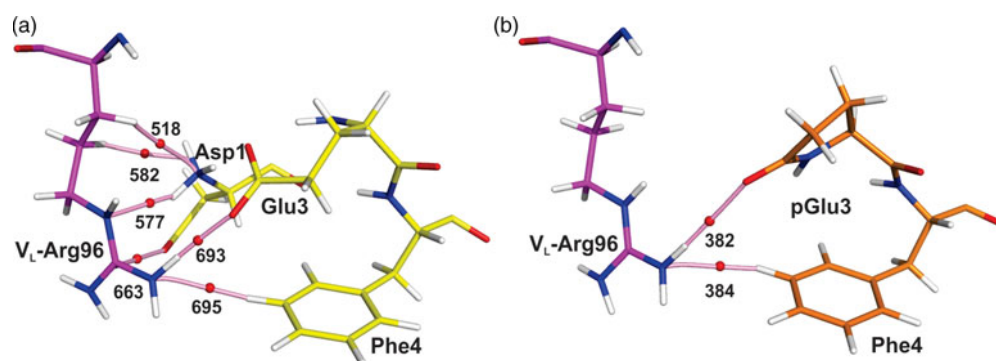


Figure 9. (Colour online) Molecular graph of the noncovalent interactions between the paratope residue (V_L -Arg96) of bapineuzumab and (a) the residues Asp1, Glu3-Phe4 of $A\beta_{WT}$ peptide (b) the residues pGlu3-Phe4 of $A\beta N3(pE)$ peptide.

3.4.2. Crystallographic water molecules involved in the binding process of $A\beta$ in the complexes

Several water molecules are located in the bind interface linking the antibody with both $A\beta$ peptides. These water molecules act as a link between the $A\beta$ peptides and the paratope. On the other hand, these molecules have different functions which may be classified as follows:

- (1) Direct bridge $A\beta$ peptides and Ab paratope.
- (2) Direct or/and indirect bridge $A\beta$ peptides and Ab paratope.

In the first case, Wat1 acts as a weak link between the $A\beta_{WT}$ peptide and Ab making a weak interaction ($O_{Wat1} \cdots HE2_{A\beta_{WT}-Phe4}$) (Figure 10(a)). In addition, Wat1 produces three interactions with the Ab; it acts as H-acceptor ($O_{Wat1} \cdots HH22_{VL-Arg96}$, $O_{Wat1} \cdots HB2_{VH-Tyr95}$) in two of them, and as an H-donor ($H2_{Wat1} \cdots OG_{VH-Ser101B}$) in the other one. Wat2 also connects the $A\beta_{WT}$ peptide directly to the antibody. This water molecule presents four hydrogen bonds where the O_{Wat2} is acting as a proton acceptor, whereas $NH3_{Asp1}$, NH_{Ala2} , $CAHA_{VL-Arg96}$ and $HG3_{VL-Arg96}$ are the proton donor counterpart (Figure 10(b)).

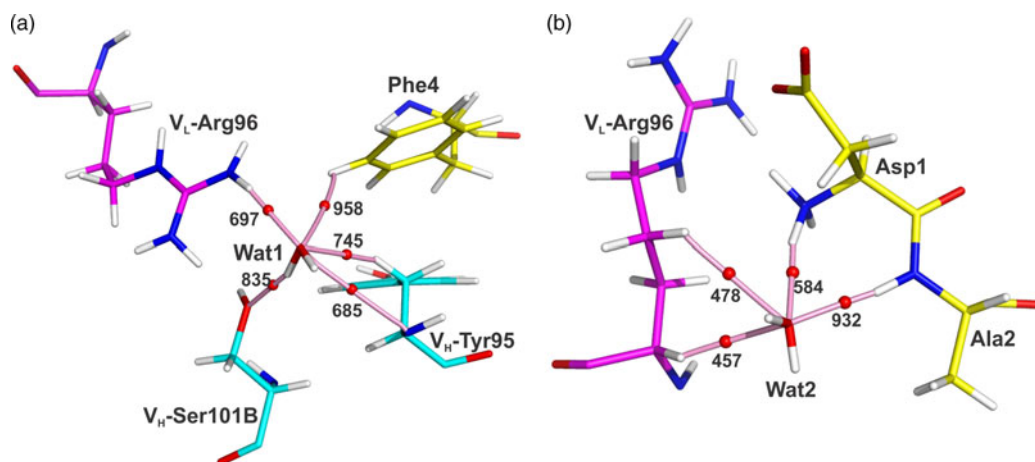


Figure 10. (Colour online) Molecular graph showing the network of interactions where (a) Wat1 acts as a link between the paratope residues (V_H -Tyr95, V_H -Ser101B, V_L -Arg96) and Phe4 of $A\beta_{WT}$ peptide (b) Wat2 acts as a link between the paratope residue (V_L -Arg96) and Asp1-Ala2 of $A\beta_{WT}$ peptide.

Another water molecule acting as a link between the different forms of $A\beta$ peptide and the Ab is Wat3. This molecule is attached to Arg5 by a moderate hydrogen bond ($O_{Wat3} \cdots HE_{A\beta_{WT}-Arg5}$) with the $A\beta_{WT}$ peptide (Figure 11 (a)), whereas $A\beta_{N3(pE)}$ peptide has two hydrogen bonds ($O_{Wat3} \cdots HE_{A\beta_{N3(pE)-Arg5}$, $O_{Wat3} \cdots HH_{21_{A\beta_{N3(pE)-Arg5}}$) (Figure 11(b)). Both peptides are linked to V_H -Tyr95 by a hydrogen bond ($O_{Wat3} \cdots HH_{V_H-Tyr95}$).

Wat4 displays hydrogen bonds with both peptides, $H2_{Wat4} \cdots OE_{1_{A\beta_{WT}-Glu3}}$ and $H2_{Wat4} \cdots OE_{A\beta_{N3(pE)-pGlu3}}$, respectively. However, while the hydrogen bond with $A\beta_{WT}$ is a strong interaction, the interaction of $A\beta_{N3(pE)}$ is a weak one. The Wat4 connects the different forms of the $A\beta$ peptides interacting with V_H -Trp47, V_L -Phe94 and

V_L -Arg96 of Ab. In both systems there is a weak interaction between the Wat4 and V_H -Trp47. Wat4 is also linked to the antibody by two interactions with V_L -Arg96 ($NH_{V_L-Arg96} \cdots O_{Wat4}$ and $HB_{2_{V_L-Arg96}} \cdots O_{Wat4}$). On the other hand, this water gives weak interactions with the amino acid V_L -Phe94 ($HD_{1_{V_L-Phe94}} \cdots O_{Wat4}$) in both complexes (Figure 12).

In group 2, Wat5 is positioned between Ala2, Glu3, Arg5 and His6, whereas Wat6 is located between V_H -Arg52 and V_H -Tyr59 forming a hydrogen bonds network that binds to both peptides with bapineuzumab. Wat5 interacts with $A\beta_{WT}$ through the residues Ala2, Glu3, Arg5 and His6 ($H1_{Wat5} \cdots O_{A\beta_{WT}-Ala2}$, $H2_{Wat5} \cdots OE_{1_{A\beta_{WT}-Glu3}}$, $H1_{Wat5} \cdots O_{A\beta_{WT}-Arg5}$, $H2_{Wat5} \cdots ND_{1_{A\beta_{WT}-His6}}$, $O_{Wat5} \cdots HB_{2_{A\beta_{WT}-$

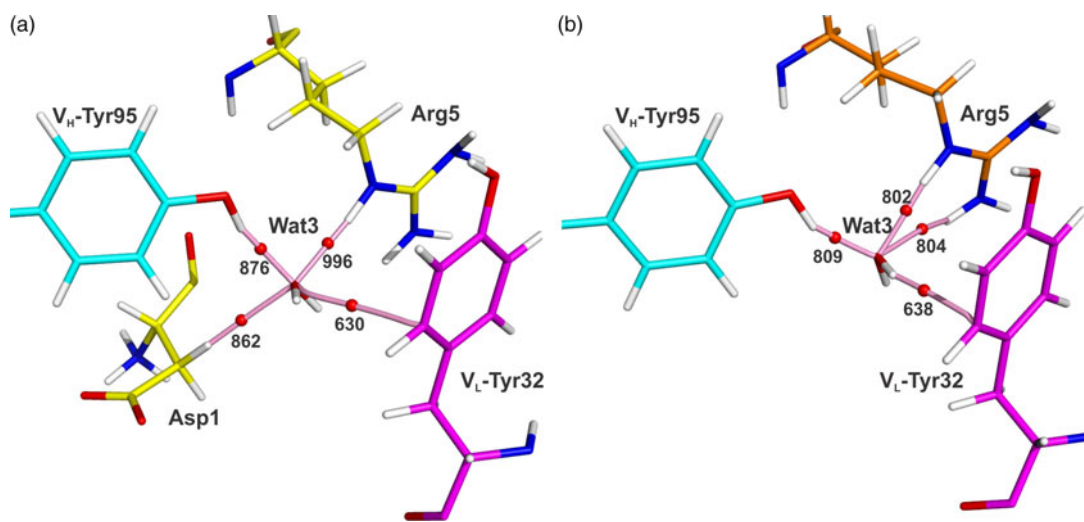


Figure 11. (Colour online) Molecular graph of the network of interactions where Wat3 acts as a link between the paratope residues (V_H -Tyr95, V_L -Tyr32) and (a) Asp1, Arg5 of $A\beta_{WT}$ peptide, (b) Arg5 of $A\beta_{N3(pE)}$ peptide.

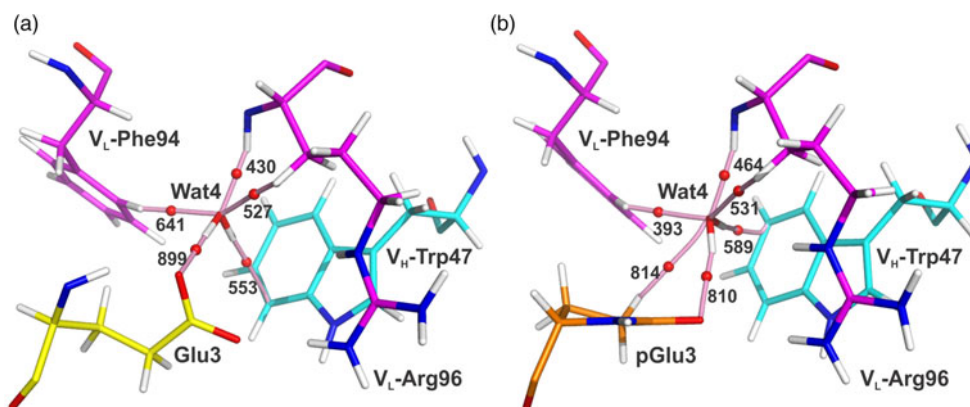


Figure 12. (Colour online) Molecular graph of the network of interactions where Wat4 acts as a link between the paratope residues (V_H -Trp47, V_L -Phe94, V_L -Arg96) and (a) Glu3 of $A\beta_{WT}$ peptide, (b) pGlu3 of $A\beta_{N3(pE)}$ peptide.

His_6) (Figure 13(a)). In the case of $A\beta_{N3(pE)}$, Wat5 interacts with the amino acids pGlu3, Arg5 and His6 ($O_{Wat5} \cdots H3_{A\beta_{N3(pE)-pGlu3}}$, $H1_{Wat5} \cdots O_{A\beta_{N3(pE)-Arg5}}$, $H2_{Wat5} \cdots ND1_{A\beta_{N3(pE)-His6}}$, $O_{Wat5} \cdots HB2_{A\beta_{N3(pE)-His6}}$) (Figure 13 (b)). In turn, Wat5 exhibits in both cases a strong hydrogen bond with the Wat6 molecule ($O_{Wat5} \cdots H1_{Wat6}$) which indirectly binds the peptides with the antibody. In addition, in $A\beta_{WT}$ complex Wat6 is strongly interacting with V_H -Arg52 and V_H -Tyr59 of bapineuzumab as well as with Glu3 ($O_{Wat6} \cdots HH21_{V_H-Arg52}$, $O_{Wat6} \cdots HH_{V_H-Tyr59}$, $H2_{Wat6} \cdots O_{A\beta_{WT}-Glu3}$). In contrast in the $A\beta_{N3(pE)}$ complex only one interaction between Wat6 and V_H -Tyr59 is observed ($O_{Wat6} \cdots HH_{V_H-Tyr59}$).

3.4.3. Comparison of the binding mode of $A\beta$ peptides and bapineuzumab

From the structural point of view, the difference between $A\beta_{WT}$ and $A\beta_{N3(pE)}$ is the lack of the amino acids Asp1 and Ala2 and the modification of Glu3 by pyro-Glu3

amino acid in $A\beta_{N3(pE)}$. This structural difference between these peptides is small, but has a drastic effect on the bapineuzumab affinity which is reflected in Figure 14. This figure shows the strength with which each residue of the $A\beta$ peptides interacts with the antibody paratope, revealing quantitatively that the residues responsible for the binding to bapineuzumab are Asp1 and Glu3.

Asp1 is the amino acid that possesses the strongest interactions with the antibody paratope. This is mainly due to the hydrogen bonds that establish the carboxylate group of Asp1 with V_H -Ser101B and V_L -Trp89 ($HE1_{V_L-Trp89} \cdots OD2_{A\beta_{WT}-Asp1}$, $H_{V_H-Ser101B} \cdots OD2_{A\beta_{WT}-Asp1}$ and $HG_{V_H-Ser101B} \cdots OD1_{A\beta_{WT}-Asp1}$). These hydrogen bonds allow bapineuzumab to capture the $A\beta_{WT}$ peptide with high efficiency. It should be noted that Asp1 is missing in $A\beta_{N3(pE)}$, being a cause of the low affinity between the antibody and $A\beta_{N3(pE)}$ peptide.

Glu3 or pGlu3 is another important residue in the recognition of the antibody paratope. This residue presents several hydrogen bonds with residues V_H -Ser50, V_H -Arg52

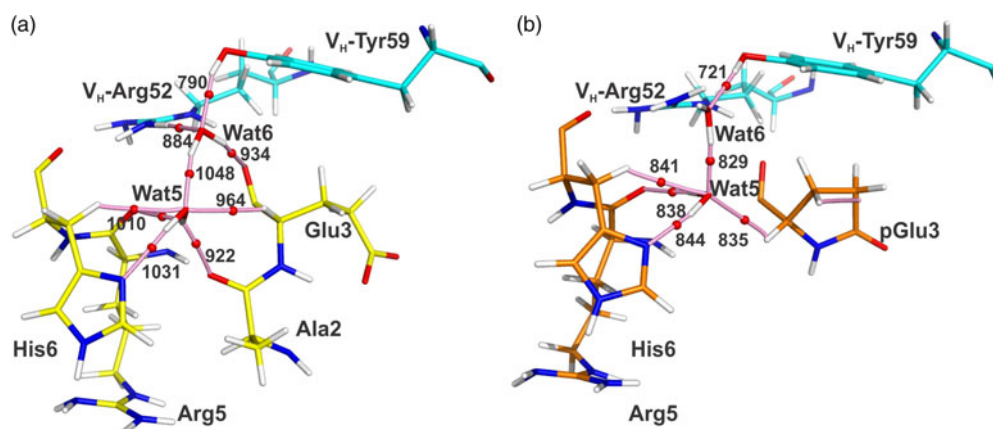


Figure 13. (Colour online) Molecular graph of the network of interactions where Wat5 and Wat6 acts as a link between the paratope residues (V_H -Arg52, V_H -Tyr59) and (a) Ala2-Glu3, Arg5-His6 of $A\beta_{WT}$ peptide, (b) pGlu3, Arg5-His6 of $A\beta_{N3(pE)}$ peptide.

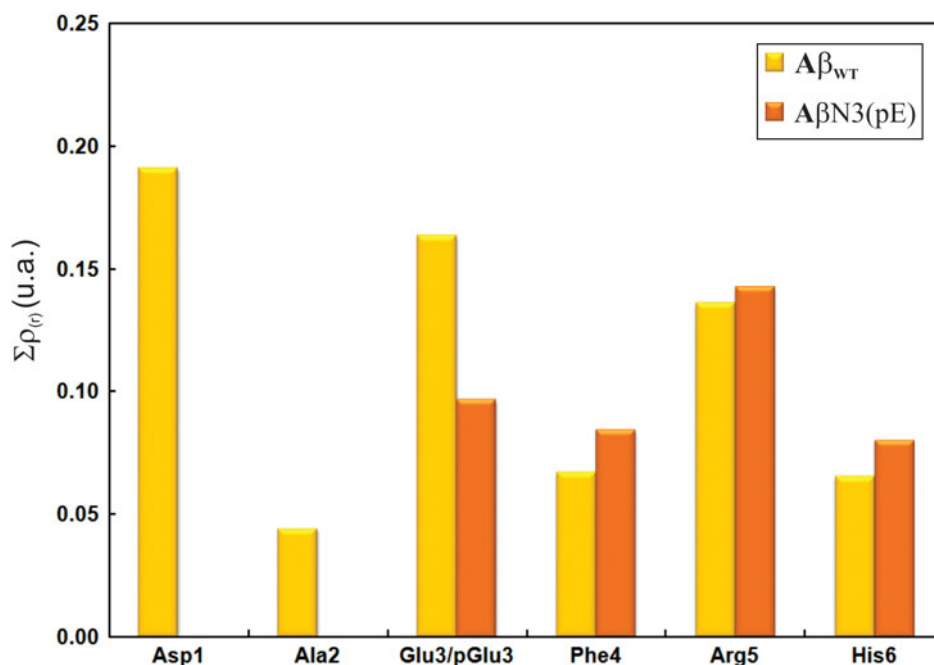


Figure 14. (Colour online) Sum of the values of charge density ($\Sigma\rho_{(r)}$) at the bond critical points for each residue of (a) A β _{WT} and (b) A β N3(pE).

and V_L-Arg96 (OH_{VH-Ser50}...O_{A β WT/A β N3(pE)-Glu3/pGlu3}, HE_{VH-Arg52}...O_{A β WT/A β N3(pE)-Glu3/pGlu3}, HH21_{VL-Arg96}...OE2_{A β WT/A β N3(pE)-Glu3/pGlu3}). These interactions occur in both complexes, but they are weaker compared to A β N3(pE)/Ab complex due to the pyroglutamate ring.

In summary, the description of the interactions established between bapineuzumab and the isoforms of A β peptide explain why the A β peptides bearing the modified Glu3 (pyro-Glu3) and without the residues Asp1 and Ala2 present low affinity for bapineuzumab.

3.4.4. Possible modifications on bapineuzumab to improve its affinity by the A β N3(pE) peptide

The QTAIM analysis is a tool important in the study of ligand–receptor interactions because the values of the electronic density at a CPB indicate the strength of the interactions. Furthermore, this technique allows us to obtain the strength of interactions of each residue of bapineuzumab interacting with the A β N3(pE) peptide and thus, we can identify which of them give the weaker interactions and therefore are good candidates to be replaced by other residues that can give stronger interactions. From Figure 3(b) it can be seen that V_H-Tyr59, V_L-Tyr32, V_L-Thr89, V_L-Phe94 and V_L-Arg96 are the residues having the weakest interactions and therefore are good candidate to be replaced by another amino acid. From the various replacements done it was found that the V_L-Tyr32Glu mutation significantly increases the affinity of bapineuzumab to A β N3(pE). V_L-Tyr32 has a value of

$\rho_{(r)} = 0.0096$ u.a., whereas the mutation V_L-Tyr32Glu presents a value of $\rho_{(r)} = 0.038$ u.a. showing a substantial increase in affinity of the bapineuzumab to A β N3(pE). It might be expected that this improvement in the affinity could have an increase in its potential therapeutic effect. However caution must be taken with this hypothesis considering the small number of mutations made in this study.

4. Conclusions

The results obtained in this study allowed us to draw interesting conclusions in two different aspects: from a methodological point of view as well as from a biological aspect. Regarding the methodological aspect, our results indicate that from relatively simple molecular modelling techniques it is possible to explain the behaviour of these two A β peptides. In this sense it is important to point out the accuracy of the combined QM/MM-QTAIM analysis, giving us a clear picture about the different binding mode of these peptides. In turn, this allowed us to identify the interactions accounting for the different affinity of these compounds. Our results contribute to the understanding of the noncovalent interactions in the context of the ligand/receptor interactions in a two-way manner, providing a detailed topological description of the interaction network of bapineuzumab with A β _{WT} and A β N3(pE) and by showing the convenience of going beyond the concept of pair-wise interactions in order to ‘see’ the electronic effects in an intricate biological environment.

With respect to the biological contribution, this study allowed us to evaluate with details the different molecular interactions that stabilise and destabilise the formation of the Ab-A β _{WT}/A β N3(pE) complexes, and therefore, to better understand why bapineuzumab might fail as a drug anti-Alzheimer. As mentioned above, all forms of A β peptides produce neuronal damage leading to the death of nerve cells. Therefore, as bapineuzumab has a higher affinity for A β _{WT} with respect to N-terminal truncated species, the last one accumulates in the brain causing cognitive decline of Alzheimer's patients. Our results indicate that interactions between the N-terminal segment of the A β _{WT} and the paratope of bapineuzumab might be responsible for the different observed affinity.

In addition, a preliminary study of point mutation was performed in this work, which suggested that replacement of V_L-Tyr32 by a Glu residue could improve the affinity between the antibody and the A β N3(pE), thereby improving its potential therapeutic effect.

Disclosure statement

No potential conflict of interest was reported by the authors.

Funding

This work was supported by Universidad Nacional de San Luis (UNSL); SECYT-Universidad Nacional del Nordeste (UNNE); CONICET (PIP 095).

Supplemental data

Supplemental material for this article can be accessed [here](#).

References

- [1] Salawu FK, Umar JT, Olokoba AB. Alzheimer's disease: a review of recent developments. *Ann Afr Med* [Internet]. Medknow Publications and Media Pvt. Ltd. 2011 Jan [cited 2014 Sep 4];10:73–79. Available from: <http://www.annalsafmed.org/article.asp?issn=1596-3519;year=2011;volume=10;issue=2;page=73;epage=79;aulast=Salawu> 2014.
- [2] De Felice FG, Wu D, Lambert MP, Fernandez SJ, Velasco PT, Lacor PN, Bigio EH, Jercic J, Acton PJ, Shughrue PJ, Chen-Dodson E, Kinney GG, Klein WL. Alzheimer's disease-type neuronal tau hyperphosphorylation induced by A beta oligomers. *Neurobiol Aging* [Internet]. 2008 [cited 2014 Sep 3];29:1334–1347. Available from: <http://www.neurobiologyofaging.org/article/S019745800700108X/fulltext> 2014.
- [3] Jin M, Shepardson N, Yang T, Chen G, Walsh D, Selkoe DJ. Soluble amyloid beta-protein dimers isolated from Alzheimer cortex directly induce Tau hyperphosphorylation and neuritic degeneration. *Proc Natl Acad Sci USA* [Internet]. 2011 [cited 2014 Jul 17];108:5819–5824. Available from: <http://www.pnas.org/content/108/14/5819> 2014.
- [4] Miles LA, Crespi GAN, Doughty L, Parker MW. Bapineuzumab captures the N-terminus of the Alzheimer's disease amyloid-beta peptide in a helical conformation. *Sci Rep* [Internet]. 2013 [cited 2014 Sep 4];3:1302. Available from: <http://www.nature.com/srep/2013/130218/srep01302/full/srep01302.html> 2014.
- [5] Sanders HM, Lust R, Teller JK. Amyloid-beta peptide Abeta3-42 affects early aggregation of full-length Abeta1-42. Peptides. [Internet]. 2009 [cited 2014 Sep 4];30:849–854. Available from: <http://www.pubmedcentral.nih.gov/articlerender.fcgi?artid=2752682&tool=pmcentrez&rendertype=abstract> 2014.
- [6] Sullivan CP, Berg EA, Elliott-Bryant R, Fishman JB, McKee AC, Morin PJ, Shia MA, Fine RE. Pyroglutamate-A β 3 and 11 colocalize in amyloid plaques in Alzheimer's disease cerebral cortex with pyroglutamate-A β 11 forming the central core. *Neurosci Lett*. [Internet]. 2011 [cited 2014 Sep 4];505:109–112. Available from: <http://www.pubmedcentral.nih.gov/articlerender.fcgi?artid=3253715&tool=pmcentrez&rendertype=abstract> 2014.
- [7] He W, Barrow CJ. The A beta 3-pyroglutamyl and 11-pyroglutamyl peptides found in senile plaque have greater beta-sheet forming and aggregation propensities *in vitro* than full-length A beta. *Biochemistry*. [Internet]. 1999 [cited 2014 Sep 4];38:10871–10877. Available from: <http://www.ncbi.nlm.nih.gov/pubmed/10451383> 2014.
- [8] Perez-Garmendia R, Gevorkian G. Pyroglutamate-modified amyloid beta peptides: emerging targets for Alzheimer's disease immunotherapy. *Curr Neuropharmacol* [Internet]. 2013 [cited 2014 Sep 4];11:491–498. Available from: <http://www.pubmedcentral.nih.gov/articlerender.fcgi?artid=3763757&tool=pmcentrez&rendertype=abstract> 2014.
- [9] D'Arrigo C, Tabaton M, Perico A. N-terminal truncated pyroglutamyl beta amyloid peptide Abeta3-42 shows a faster aggregation kinetics than the full-length A beta1-42. *Biopolymers* [Internet]. 2009 [cited 2014 Sep 4];91:861–873. Available from: <http://www.ncbi.nlm.nih.gov/pubmed/19562755>
- [10] Nussbaum JM, Schilling S, Cynis H, Silva A, Swanson E, Wangsanut T, Tayler K, Wiltgen B, Hatami A, Röncke R, Reymann K, Hutter-Paier B, Alexandru A, Jagla W, Graubner S, Glabe CG, Demuth H-U, Bloom GS. Prion-like behaviour and tau-dependent cytotoxicity of pyroglutamylated amyloid- β . *Nature* [Internet]. 2012 [cited 2014 Aug 28];485:651–655. Available from: <http://dx.doi.org/10.1038/nature11060> 2014.
- [11] Harigaya Y, Saido TC, Eckman CB, Prada CM, Shoji M, Younkin SG. Amyloid beta protein starting pyroglutamate at position 3 is a major component of the amyloid deposits in the Alzheimer's disease brain. *Biochem Biophys Res Commun* [Internet]. 2000 [cited 2014 Sep 4];276:422–427. Available from: <http://www.sciencedirect.com/science/article/pii/S0006291X00934909> 2014.
- [12] Kuo YM, Emmerling MR, Woods AS, Cotter RJ, Roher AE. Isolation, chemical characterization, and quantitation of A beta 3-pyroglutamyl peptide from neuritic plaques and vascular amyloid deposits. *Biochem Biophys Res Commun*. [Internet]. 1997 [cited 2014 Sep 4];237:188–191. Available from: <http://www.ncbi.nlm.nih.gov/pubmed/9266855> 2014.
- [13] Sperling R, Salloway S, Brooks DJ, Tampieri D, Barakos J, Fox NC, Raskind M, Sabbagh M, Honig LS, Porsteinsson AP, Lieberburg I, Arrighi HM, Morris KA, Lu Y, Liu E, Gregg KM, Brashear HR, Kinney GG, Black R, Grundman M. Amyloid-related imaging abnormalities in patients with Alzheimer's disease treated with bapineuzumab: a retrospective analysis. *Lancet Neurol*. ;11:241–249. Available from: [http://dx.doi.org/10.1016/S1474-4422\(12\)70015-7](http://dx.doi.org/10.1016/S1474-4422(12)70015-7) 2012.
- [14] Watt AD, Crespi GAN, Down RA, Ascher DB, Gunn A, Perez KA, Mclean CA, Villemagne VL, Parker MW, Barnham KJ, Miles LA. Do current therapeutic anti-a β antibodies for Alzheimer's disease engage the target?. *Acta Neuropathol*. 2014;127(6):803–810. doi: 10.1007/s00401-014-1290-2.
- [15] Gardberg A, Dice L, Pridgen K, Ko J, Patterson P, Ou S, Wetzel R, Dealwis C. Structures of A β -related peptide–monoclonal antibody complexes. *Biochemistry*. [Internet]. 2009 [cited 2014 Sep 4];48:5210–5217. Available from: <http://dx.doi.org/10.1021/bi9001216> 2014.
- [16] Case DA, Cheatham TE, Darden T, Gohlke H, Luo R, Merz KM, Onufriev A, Simmerling C, Wang B, Woods RJ. The Amber biomolecular simulation programs. *J Comput Chem*. [Internet]. 2005 [cited 2012 Jul 18];26:1668–1688. Available from: <http://www.pubmedcentral.nih.gov/articlerender.fcgi?artid=1989667&tool=pmcentrez&rendertype=abstract> 2012.
- [17] Lindorff-Larsen K, Piana S, Palmo K, Maragakis P, Klepeis JL, Dror RO, Shaw DE. Improved side-chain torsion potentials for the

- Amber ff99SB protein force field. Proteins. [Internet]. 2010 [cited 2012 Jul 23];78:1950–1958. Available from: <http://www.pubmedcentral.nih.gov/articlerender.fcgi?artid=2970904&tool=pmcentrez&rendertype=abstract> 2012.
- [18] Izaguirre JA, Catarello DP, Wozniak JM, Skeel RD. Langevin stabilization of molecular dynamics. J Chem Phys. [Internet]. 2001 [cited 2012 Aug 22];114:2090. Available from: <http://link.aip.org/link/?JCP/A6/114/2090/1> 2012.
- [19] Essmann U, Perera L, Berkowitz ML, Darden T, Lee H, Pedersen LG. A smooth particle mesh Ewald method. J Chem Phys. 1995; 103:31–34.
- [20] Onufriev A, Bashford D, Case DA. Modification of the generalized born model suitable for macromolecules. J Phys Chem B. [Internet]. 2000 [cited 2012 Oct 17];104:3712–3720. Available from: <http://dx.doi.org/10.1021/jp994072s> 2012.
- [21] Cornell WD, Cieplak P, Bayly CI, Gould IR, Merz KM, Ferguson DM, Spellmeyer DC, Fox T, Caldwell JW, Kollman PA. A second generation force field for the simulation of proteins, nucleic acids, and organic molecules. J Am Chem Soc. 1995;117(19):5179–5197. doi:10.1021/ja00124a002.
- [22] Wang J, Wolf RM, Caldwell JW, Kollman PA, Case DA. Development and testing of a general amber force field. J Comput Chem. 2004;25(9):1157–1174. doi:10.1002/jcc.20035.
- [23] Boys SF, Bernardi F. The calculation of small molecular interactions by the differences of separate total energies. Some procedures with reduced errors. Mol Phys. 1970;19(4):553–566. doi:10.1080/00268977000101561.
- [24] Simon S, Duran M, Dannenberg JJ. How does basis set superposition error change the potential surfaces for hydrogen-bonded dimers? J Chem Phys. 1996;105(24):11024. doi:10.1063/1.472902.
- [25] Saen-oon S, Kuno M, Hannongbua S. Binding energy analysis for wild-type and Y181C mutant HIV-1 RT/8-Cl TIBO complex structures: quantum chemical calculations based on the ONIOM method. Proteins. 2005;61(4):859–869. doi:10.1002/prot.20690.
- [26] Frisch MJ, Trucks GW, Schlegel HB, Scuseria GE, Robb MA, Cheeseman JR, Scalmani G, Barone V, Mennucci B, Petersson GA, Nakatsuji H, Caricato M, Li X, Hratchian HP, Izmaylov AF, Bloino J, Zheng G, Sonnenberg JL, Hada M, Ehara M, Toyota K, Fukuda R, Hasegawa J, Ishida M, Nakajima T, Honda Y, Kitao O, Nakai H, Vreven T, Montgomery JA Jr, Peralta JE, Ogliaro F, Bearpark M, Heyd JJ, Brothers E, Kudin KN, Staroverov VN, Kobayashi R, Normand J, Raghavachari K, Rendell A, Burant JC, Iyengar SS, Tomasi J, Cossi M, Rega N, Millam JM, Klene M, Knox JE, Cross JB, Bakken V, Adamo C, Jaramillo J, Gomperts R, Stratmann RE, Yazyev O, Austin AJ, Cammi R, Pomelli C, Ochterski JW, Martin RL, Morokuma K, Zakrzewski VG, Voth GA, Salvador P, Dannenberg JJ, Dapprich S, Daniels AD, Farkas Ö, Foresman JB, Ortiz JV, Cioslowski J, Fox DJ. Gaussian 09. Wallingford, CT: Gaussian, Inc.; 2009.
- [27] Bader RFW. Atoms in molecules. Acc Chem Res. 1985;18(1):9–15. doi:10.1021/ar00109a003.
- [28] Lu T, Chen F. Multiwfn: a multifunctional wavefunction analyzer. J Comput Chem. 2012;33(5):580–592. doi:10.1002/jcc.22885.